Impact Analysis of Informatization Means Driven by Artificial Intelligence Technology on Visual Communication

Lei Ni
School of Art and Design, Yellow River Conservancy Technical Institute, Kaifeng 475004, China

***Abstract*—With the popularization of computer technology, the combination of artificial intelligence and image processing technology has become a research hotspot in the visual communication. Image processing technology mostly involves segmentation and detection of images. Image segmentation often focuses on extracting image contour information, while ignoring the color of the image. The calculation time for image detection is relatively long, and the calculation steps are also relatively cumbersome. In response to the above issues, a density peak clustering algorithm was proposed for image segmentation. In the phase of image detection, the region recommendation network is introduced to improve the faster region Convolutional neural network algorithm. The findings demonstrate that under 15% Gaussian noise and 10% Salt-and-pepper noise, the segmentation accuracy of the density peak clustering algorithm is 98.13% and 97.89% respectively. The accuracy, recall and F-measure of the improved fast region Convolutional neural network algorithm are 98.49%, 97.29% and 97.77% respectively. The accuracy and average time consumption in the graphics processor environment are 98.18% and 2.94ms, respectively. In conclusion, the image segmentation algorithm based on density peak clustering algorithm and the improved fast region Convolutional neural network algorithm are robust, which have good segmentation and detection effects.**

***Keywords*—Image segmentation; image detection; density peak clustering algorithm; convolutional neural network; faster region convolutional neural network**

I. Introduction

A. Research Background

With the continuous progress of science and technology,the Visual communication is also seeking breakthroughs [1-2]. As a common form of visual communication, the processing technology of images has also shifted from artificial to intelligent [3]. Especially in today's increasingly popular digital information processing and transmission, images, as the most intuitive form of visual expression, have become an indispensable part of information communication. Image processing technology includes image digitization, image enhancement and restoration, image data encoding, image segmentation (IS), and image detection technology. Covering various aspects from image acquisition, image analysis to image understanding, the progress of these technologies directly promotes the rapid development of application fields such as medical imaging, autonomous driving, intelligent security, entertainment media, etc. [4]. As a key link in image processing technology, image segmentation and detection are becoming increasingly important. Among them, IS technology divides an image into several specific and unique regions. Then the area is extracted and displayed independently [5-7]. The application of this technology can help computers identify and extract regions of interest in images, while image detection technology determines their categories and locations through further analysis and localization of these regions. Image detection technology refers to IS based on target geometry and statistical features. Furthermore, the segmentation and recognition of the target are combined to determine the location and size of the target [8]. In recent years, with the introduction of deep learning algorithms, especially the successful application of convolutional neural networks (CNN) in image processing, the accuracy and speed of image segmentation and detection have been greatly improved. Meanwhile, emerging technologies such as convolutional neural networks combined with region recommendation networks also provide broad space for further optimizing image processing.

B. Existing Issues

Although deep learning has made significant progress in image segmentation and detection, there are still some issues that need to be addressed urgently. First, traditional IS algorithms often use image contour information to extract regions of interest in images. The importance of color information in images is ignored, resulting in computational redundancy. Traditional image detection algorithms are mostly based on the depth CNN to detect image objects. Its computation takes a long time, which can easily lead to computational redundancy and a large amount of memory occupation, resulting in slow image object detection speed. Secondly, the widely used convolutional neural networks have a large computational load and slow detection speed when processing image detection. Due to the complexity of convolution operations, especially when generating candidate regions, a large number of redundant computational steps can lead to excessive memory consumption and significantly increased processing time, making it difficult to meet real-time requirements [9]. In addition, existing algorithms perform poorly in processing images with high noise or complex backgrounds, easily losing key details and leading to a decrease in detection accuracy. Finally, some existing image segmentation and detection methods mostly rely on the specific distribution of data, and the algorithm has poor universality to the dataset. The robustness and adaptability of algorithms still need to be improved when facing different application scenarios or data types. Especially in practical applications, the

*Corresponding Author.

diversity and complexity of image data pose higher requirements for algorithms. Therefore, designing an algorithm that can simultaneously handle multiple complex situations, improve segmentation and detection accuracy, and has efficient computing capabilities has become an important research direction in the field of visual communication.

C. Research Content and Innovative Points

In response to the above issues, based on the low requirement for data distribution and simple principle of the Density Peak Clustering (DPC), the image center information and color information are extracted separately for IS work to obtain the DPC-IS algorithm. In order to achieve the image detection target, the fast-regional Convolutional neural network (FastR-CNN) algorithm is improved by introducing the regional recommendation network. The innovation points of the research mainly include the following two points. Firstly, DPC-IS algorithm is used to extract the center information and color information, which is convenient for Hierarchical clustering of pixels in the image. Then, based on the FastR-CNN algorithm, a regional recommendation network is introduced to reduce computational redundancy and improve detection accuracy and speed. The research structure contains four parts. The first is a review of relevant research results. The second is the DPC-IS algorithm and the FasterR-CNN algorithm construction. The third part is to verify the availability of the IS and image detection. The final part is a summary.

II. Related Work

IS is an important image-processing technology. The purpose is to segment the image into practical and non-interference regions. Objects of interest in the area can be displayed independently from the Background independence. As a hotspot direction in computer vision, how to apply IS technology to different professional fields has been deeply explored by many scholars. Shi et al. designed a fuzzy contour model based on multi-channel CNN to enhance the segmentation accuracy of medical images. The findings demonstrate that the model has good segmentation performance and robustness [10]. Liu et al. designed an IS algorithm based on deep learning network to identify the particle size distribution of crushed ore. Firstly, this algorithm was applied to preprocess the raw ore images. Then, deep learning networks were used to generate optimization model. The feasibility of this algorithm has been verified through simulation experiments [11]. Ji proposed a Level set algorithm based on significant fitting energy to solve the noise and non-uniformity of gray levels in image segmentation. This algorithm introduced a distance regularization term to eliminate the reinitialization process. Simulation experiments show that the algorithm has good segmentation ability in visual perception [12]. To improve the noise resistance and discrimination of segmented images with uneven grayscale, Li et al. designed a Bayesian criterion based on image segmentation. Local prior region descriptions were used to characterize image regions. From the simulation experiment, this method has superior performance in time efficiency and noise robustness [13]. Biswas et al. proposed a segmentation image active contour model to improve the image segmentation effect by combining the local binary fitting energy function and the improved Laplacian Gaussian function energy function. The findings indicate that the active contour model has good performance in segmentation accuracy, F-value, and Central Processing Unit (CPU) execution time [14].

Image detection technology is another important means in image processing technology. The purpose is to enable computers to automatically recognize target categories in images. By drawing a bounding box around the target, the position of each target is labeled. Chen proposed a license plate recognition model based on CNN and K-means clustering segmentation to address the recognition difficulties caused by uneven license plate form, color, viewpoint, and lighting environment. From the findings, this model can improve the recognition and detection accuracy [15]. Vinolin et al. proposed a deep CNN based on Taylor rider optimization algorithm for detecting concatenated images. Compared with traditional detection algorithms, precision measurement accuracy has been significantly improved [16]. Based on the fast CNN model, Luo et al. introduced neural architecture search optimization and feature enrichment to achieve multi-scale vehicle target detection in traffic scenes. From the findings, the robustness of the detection method is effectively improved [17]. Ramaraj proposed a face image detection algorithm based on CNN with Long short-term memory, aiming at the difficulty of face image detection caused by facial occlusion and low resolution. The research results confirm that the detection algorithm has superior performance and good detection accuracy [18]. Joy et al. constructed a fast-regional CNN multi object detection method based on incremental classification in the monitoring field. This detection method was mainly divided into class incremental learning part and domain adaptive part. The experimental results confirm that this method performs well on challenging targets including lighting changes, shadows, partial occlusion, and dynamic backgrounds [19].

To summarize, in image processing technology, there are rich research achievements in IS algorithm and image detection algorithm. But most IS algorithms only utilize the contour information of the image, ignoring the importance of the color information of the image. Most image detection algorithms require a significant amount of time when generating candidate regions through selective search. This process will generate a large number of invalid regions, resulting in wasted computing power. To address the above issues, a DPC-IS algorithm is constructed for IS based on spatial color distribution. The FasterR-CNN algorithm is constructed to detect target images.

III. DPC-IS Algorithm Design and FasterR-CNN Algorithm Construction

As a visual communication medium, images can express information in the most intuitive and authentic way. Therefore, compared to other media, images convey a richer amount of information. To process images more intuitively, DPC-IS algorithm and FasterR-CNN algorithm are used for segmentation and detection. This chapter focuses on the DPC-IS algorithm design and the FasterR-CNN algorithm construction in image detection.

A. Design of DPC-IS Algorithm in Image Segmentation

In Visual communication, image is not only a widely used form, but also a unique data format. Pixels are evenly arranged in the image space. Each pixel carries a unique color label. And each pixel has two features, namely spatial position feature (X,Y) and color feature (R,G,B). The spatial and color features are uniformly set to 1 dimension. The spatial and color features are merged to form a two-dimensional space. A two-dimensional sparse matrix (i,j) is used to represent an image. The value of matrix (i,j) is 0 or 1, indicating whether the pixel value of image i is j, as shown in Fig. 1.

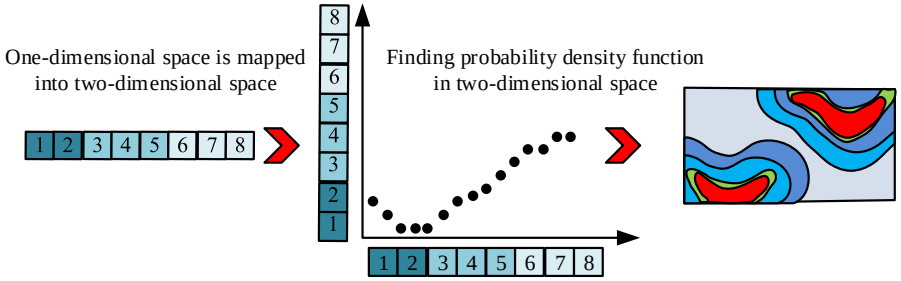

Fig. 1. The 1-dimensional space is mapped to the 2-dimensional space and the distribution of probability density function is obtained.

After obtaining the two-dimensional spatial distribution position of image pixels in Fig. 1, the kernel probability density function is used to measure the distribution of pixel points. For a set $\{X_1, X_2, \cdots, X_n\}$ with n sample points, the probability density function $f_g(x)$ of a certain point is equal to the sum of the influences of all data samples at that point, as shown in Eq. (1)

$$f_g(x) = \frac{1}{nh}\sum_{i=1}^{n} K\left(\frac{X - X_i}{h}\right) \tag{1}$$

In Eq. (1), n is the sample points. K represent the kernel function. h is the window width. When using kernel functions to estimate the probability density function, the distance $d\left(\left|P_i, P_j\right|\right)$ between data points P_i and P_j in the 5-dimensional space (X,Y,R,G,B) needs to be defined, as shown in Eq. (2).

$$d\left(\left|P_i, P_j\right|\right) = \sqrt{\left(\frac{d_s}{\alpha_s}\right)^2 + \left(\frac{d_c}{\alpha_c}\right)^2} \tag{2}$$

In Eq. (2), d_s and d_c represent spatial distance and color distance, respectively. α_s and α_c are spatial smoothing parameters and color smoothing parameters, respectively. The values of α_s and α_c need to be manually set. The expression of spatial distance d_s is shown in Eq. (3).

$$d_s = \sqrt{\left(x_i - x_j\right)^2 + \left(y_i - y_j\right)^2} \tag{3}$$

In Eq. (3), x_i and x_j represent the horizontal distances of i and j. y_i and y_j stands for the vertical distances of i and j, respectively. The color distance d_c is expressed as an approximate CIElab color distance, as shown in Eq. (4).

$$dc = \sqrt{\left(2 + \frac{\bar{r}}{256}\right) \times \Delta R^2 + 4 \times \Delta G^2 + \left(2 + \frac{255 - \bar{r}}{256}\right) \times \Delta B^2} \tag{4}$$

In Eq. (4), ΔR, ΔG and ΔB stands for the weighted Euclidean distances of red, green, and blue, respectively. $\bar{r}$ refers to the average level of red. The expressions of ΔR, ΔG and ΔB are shown in Eq. (5).

$$\begin{cases} \Delta R = r_i - r_j \\ \Delta G = g_i - g_j \\ \Delta B = b_i - b_j \end{cases} \tag{5}$$

In Eq. (5), r_i and r_i represent the red distances of i and j. g_i and g_j stands for the green distances of i and j. b_i and b_j represent the blue distances of i and j, respectively. The probability density function f of the kernel function is shown in Eq. (6).

$$f = \frac{1}{n}\sum \exp\left(\frac{d_s^{\,2}}{\alpha_s^{\,2}} + \frac{d_c^{\,2}}{\alpha_c^{\,2}}\right) \tag{6}$$

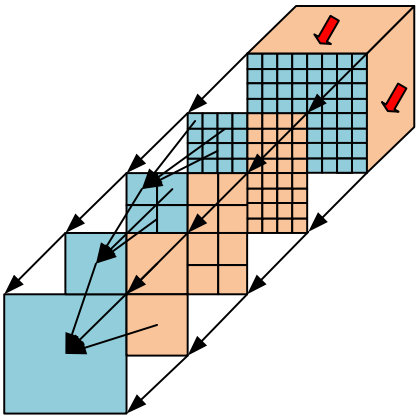

Fig. 2. Schematic diagram of the reduction algorithm.

To reduce the computational complexity of the probability density function in 5-dimensional space, CUDA programming was used to accelerate graphics processing unit (GPU) operations on images. Color information is mapped to a 2D image. The protocol algorithm is used to search for color points with the maximum probability density function value. The color of this point and the corresponding function values are output to the density map and color map, respectively. Fig. 2 depicts the protocol algorithm [20-21].

The constraint algorithm in Fig. 2 follows the CUDA setting for finding the probability density function. For the 3D color space corresponding to the original pixel Block, the maximum value of Thread in 16 color spaces is calculated sequentially, transforming the 3D color space into a 2D color space. Recursively compare the density values of four positions in a two-dimensional color space. The maximum values of the four positions are passed to the next layer of color space until the maximum density value in the three-dimensional color space is finally determined. The density map containing contour information estimated by the spatial color probability density function has unclear boundaries. Therefore, a non-maximum suppression algorithm is adopted to refine the image boundary contour and apply it to IS [22]. Traditional algorithms only use image contour information and ignore image color information, resulting in the inability to specify segmentation levels. The DPC algorithm was applied to IS work to obtain the DPC-IS algorithm. DPC is a clustering algorithm based on center points. The local density ld of the sample points is used to define the clustering center t and the nearest distance md. The local density ld_i of sample point i is illustrated in Eq. (7) [23].

$$ld_i = \sum_j \chi\left(d\left(i,j\right) - d_c\right) \tag{7}$$

In Eq. (7), $d\left(i,j\right)$ stands for the Euclidean distance between samples i and j. d_c stands for the cutoff distance. When $x<0$, $\chi\left(x\right)=1$. Otherwise, the value is 0. The expression of cluster center t_i is illustrated in Eq. (8).

$$t_i = \arg\min_{j:ld_j > ld_i}\left(d\left(i,j\right)\right) \tag{8}$$

In Eq. (8), ld_j refers to the local density of sample point j. The $\arg\min$ function refers to the value of a variable when $d\left(i,j\right)$ reaches the minimum value. The segmentation effect varies with the number of cluster centers, as shown in Fig. 3.

Fig. 3 shows the segmentation results with clustering centers of 2, 5, 7, 12, 14, and 20, respectively. As the number of clustering centers increases, the regions segmented by the DPC-IS algorithm are also increasing. The segmentation details are gradually improving. The nearest distance md_i of sample point i is shown in Eq. (9).

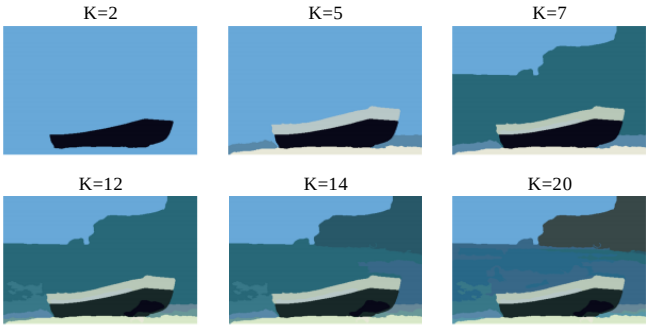

Fig. 3. Schematic diagram of segmentation effect of different clustering centers.

$$md_i = \min_{j:ld_j > ld_i} d\left(i,j\right) \tag{9}$$

When the DPC algorithm is applied to IS, the previously obtained density map containing pixel distribution center information can be directly used as the local density of pixels. The nearest distance of pixel point k is shown in Eq. (10).

$$md_k = \min d_c\left(i,j\right) \tag{10}$$

In Eq. (10), pixels l and k are segmented adjacent. $ld_l > ld_k$. The definition of adjacent segmentation is that if two pixels are adjacent, the segmentation area to which the two pixels belong is adjacent.

B. Construction of FasterR-CNN Algorithm in Image Detection

The CNN model, as a fresh neural network model, is extensively applied in image processing. Unlike traditional neural network models, CNN models add many feature learning components to the existing network. The hidden layer is reasonably divided into convolutional layer and pooling layer, in order to directly use convolutional layer to train image data. The features of interested objects in the graph are extracted, reducing the computational workload of object detection. The CNN model structure is shown in Fig. 4.

Fig. 4 depicts the essential framework of the CNN model. It mainly consists of a series of convolutional layers, incentive layers, pooling layers, and fully connected layers (FCL). The expression of convolutional layer is shown in Eq. (11).

$$x_n^l = f\left(\sum_{i\in G_n} x_m^{l-1} * Kernel_{mn}^l + a^l\right) \tag{11}$$

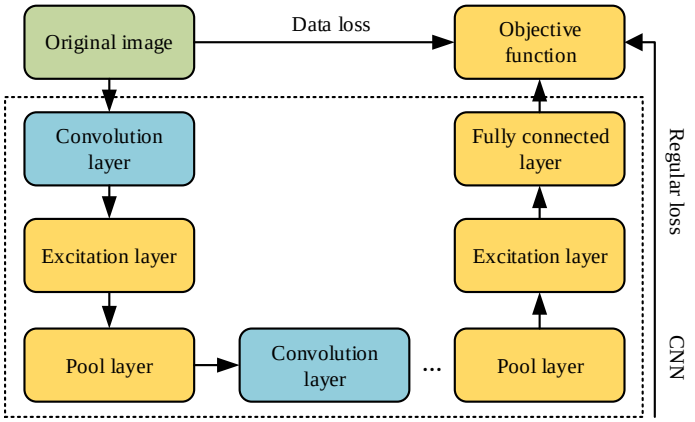

Fig. 4. Schematic diagram of CNN model structure.

In Eq. (11), x_n^l represents the m-th neuron in the l-th layer. *Kernel* refers to the convolutional kernel of the layer. b is the bias term. * represents convolutional operations. G_n represents the number of inputs for the n-th neuron. $f(\square)$ is the nonlinear excitation function. The CNN model has local connectivity. Therefore, each neuron can only perceive a portion of the image, effectively reducing the interaction between neurons and computational complexity. Additionally, the same feature may exist at different locations in the image. The convolutional layer adopts a parameter sharing method, so that each convolutional kernel corresponds to a type of feature, thereby reducing the required parameters for training. The excitation layer introduces nonlinear features into the neural network, enabling it to approximate any nonlinear function. This effectively enhances the feature expression ability of CNN models. The commonly used expression of the excitation function is shown in Eq. (12).

$$\begin{cases} f_S(x) = \dfrac{1}{1+e^{-x}} \\ f_T(x) = \dfrac{e^{x}-e^{-x}}{e^{x}+e^{-x}} \\ f_R(x) = \begin{cases} x, x \geq 0 \\ 0, x < 0 \end{cases} \end{cases} \tag{12}$$

In Eq. (12), $f_S(x) = \dfrac{1}{1+e^{-x}}$ is sigmoid function. $f_T(x) = \dfrac{e^{x}-e^{-x}}{e^{x}+e^{-x}}$ is the Tanh function. $f_R(x) = \begin{cases} x, x \geq 0 \\ 0, x < 0 \end{cases}$ is ReLU function. The output of neurons is mapped to the $(0,1)$ interval through the sigmoid function. However, this function has a soft saturation characteristic, which can cause gradient disappearance in deep networks. The average output value of the Tanh function is closer to 0. It has good convergence, but still cannot solve the gradient disappearance. The ReLU function sets the output values of some neurons to 0, making the neural network sparse. To some extent, the problem of overfitting has been avoided. In addition, the derivative of the positive activation value of the ReLU function is 1, which can effectively avoid gradient disappearance. Therefore, ReLU function is used as the activation function of the excitation layer [24]. The pooling layer commonly uses maximum pooling and mean pooling to reduce the dimensionality of feature maps. The network parameters and computational complexity are reduced to facilitate feature compression, as shown in Fig. 5.

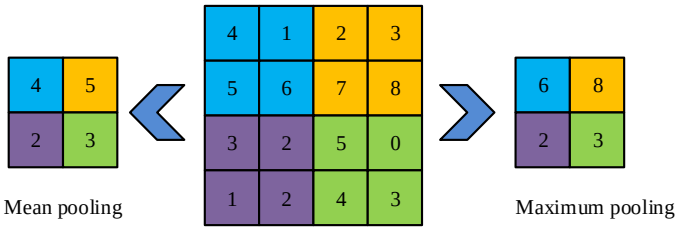

Fig. 5. Mean pool and maximum pool.

The feature data obtained from mean pooling in Fig. 5 is relatively sensitive to texture information. Maximizing pooling places more emphasis on background information. The function of the FCL is to integrate the features of the input image. The feature maps generated by convolutional layers are mapped into fixed length feature vectors to complete image classification tasks. The calculation of the FCL is shown in Eq. (13).

$$x_n^l = f\left(\sum_{i \in G_n} x_m^{l-1} * w_{m,n} + a_n\right) \tag{13}$$

In Eq. (13), x_n^l refers to the output neuron of the FCL. $w_{m,n}$ and a_n represent the weights and offsets between neurons, respectively. The image classification task requires adding a classifier after the high-dimensional feature vectors of the FCL. The feature vectors of the FCL are mapped to the probability of each category. The category with the highest probability is the classification result. The expression of function $g_\theta(x)$ is shown in Eq. (14).

$$g_\theta(x^i) = \frac{1}{\sum_{n=1}^{k} e^{\theta_n^T x^n}} \begin{bmatrix} e^{\theta_1^T x^n} \\ e^{\theta_2^T x^n} \\ \cdots \\ e^{\theta_n^T x^n} \end{bmatrix} \tag{14}$$

In Eq. (14), $\theta = \left[\theta_1^T \theta_2^T \cdots \theta_n^T\right]$ is the learning parameter of the classifier, including the Softmax cost function $F(\theta)$ of the weight penalty term, as shown in Eq. (15).

$$F(\theta) = -\frac{1}{i}\left[\sum_{m=1}^{k}\sum_{n=1}^{k}\{y^m = n\}\log\frac{e^{\theta_n^T x^m}}{\sum_{l=1}^{k} e^{\theta_l^T x^m}}\right] + \frac{\beta}{2}\sum_{m=1}^{k}\sum_{n=0}^{j}\theta_{mn}^2 \tag{15}$$

In Eq. (15), i is the samples. β is the coefficient of the regularization term. In the training process, CNN uses the Gradient descent to minimize $F(\theta)$, so as to find the optimal solution of parameter weight θ. Traditional regional CNN models consume a long amount of computation time when performing object detection. It is easy to cause computational redundancy and a large amount of memory consumption, resulting in slow target detection speed. To improve the detection accuracy and speed of graphics, the FasterR-CNN has been introduced. The FasterR-CNN algorithm is a deep learning algorithm that introduces regional recommendation networks to improve fast regional CNN networks. This algorithm utilizes convolutional network training to achieve target detection without any other algorithm operations. The selective search algorithm in regional recommendation networks is different from that in traditional regional CNN models. This method uses the feature map extracted from the last layer of CNN as the input feature. Convolutional kernels are used to move within the feature map and output suggestion boxes. Every time the convolution kernel moves, it will take the central position of the window as the base point to build nine anchor windows with different sizes and different Aspect ratio. It is mapped into the image to form a feature vector. Then the FCL is applied for classification and positioning. The FasterR-CNN algorithm structure is shown in Fig. 6.

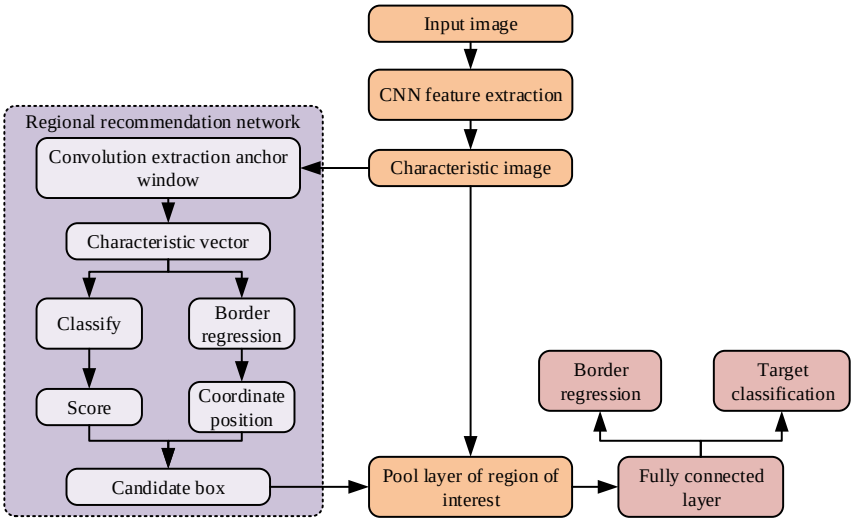

Fig. 6. FasterR-CNN algorithm flow diagram.

The algorithm flow in Fig. 6 is as follows. Firstly, the input image is extracted using CNN for feature extraction. Then input the extracted feature images into the region recommendation network for candidate border generation. The region border and feature map classify and locate the objective function through the pooling layer of interest in the fast region CNN network. The final image target detection effect is obtained.

IV. Result Analysis of 3DPC-IS Algorithm and FasterR-CNN Algorithm

To better validate the feasibility of the DPC-IS algorithm and FasterR-CNN algorithm, multiple control groups are set up in the BSDS500 database and Matlab simulation software for comparative experiments. This chapter focuses on the performance of DPC-IS algorithm and FasterR-CNN algorithm.

A. Performance Analysis of DPC-IS Algorithm

To prove the effectiveness of the DPC-IS algorithm, comparative experiments are designed using Simple Linear Iterative Clustering (SLIC), Fast Partitioning of Vector Value Images (FPVVI) algorithm, Normalized Cuts (NC) algorithm, and DPC-IS algorithm. The performance indicator is IS accuracy. The experimental platform is the BSDS500 database.

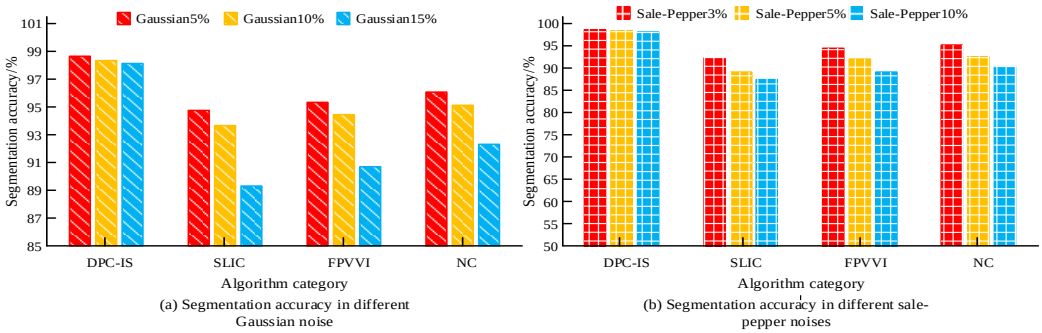

Fig. 7. Segmentation accuracy of four algorithms under different noise categories.

Fig. 7 depicts the segmentation accuracy of four algorithms in different noise categories. Fig. 7(a) depicts the segmentation accurac of four algorithms in different Gaussian noise categories. When the Gaussian noise is 5%, the segmentation accuracy of PDC algorithm is 98.65%. The SLIC, FPVVI, and NC algorithms are 94.75%, 95.33%, and 96.07%, respectively. When the Gaussian noise is 15%, the PDC, SLIC, FPVVI and NC algorithms are 98.13%, 89.31%, 90.69% and 92.31% respectively. Fig. 7(b) illustrates the segmentation accuracy of four algorithms in different Salt-and-pepper noise categories. When Salt-and-pepper noise is 3%, the segmentation accuracy of PDC algorithm is 98.45%. The SLIC, FPVVI, and NC algorithms are 92.15%, 94.32%, and 94.99%, respectively. When the Salt-and-pepper noise is 10%, the PDC, SLIC, FPVVI, and NC algorithms are 97.89%, 87.32%, 89.05%, and 90.12%, respectively. The research results show that as the media of Visual communication, the PDC algorithm has superior performance in the processing.

Fig. 8. Segmentation effect of four algorithms on some images.

The segmentation effects of the four algorithms on some images are shown in Fig. 8, Fig. 8(a) to Fig. 8(e) show the segmentation effects of the original image, DPC-IS algorithm, FPVVI algorithm, SLIC algorithm, and NC algorithm, respectively. The DPC-IS algorithm can effectively segment images. Compared to FPVVI, SLIC, and NC algorithms, the DPC-IS algorithm filters the background while retaining the main salient regions. Important areas are displayed separately from the background, making the visual communication effect more prominent. To assess the effectiveness in segmenting images, three performance indicators were introduced: Variance of Information (VI), Probabilistic Rand Index (PRI), and Segmentation Coverage (SC). VI is the difference between the segmentation and the benchmark result. The smaller the value, the better. The higher the values of PRI and SC, the better the performance.

Table I shows the PRI, VI, and SC results of the two algorithms. The Optimal Dataset Scale (ODS) and Optimal Image Scale (OIS) represent the optimal result thresholds within the database and the optimal result thresholds for each image, respectively. The PRI values of DPC-IS algorithm under ODS and OIS are 0.831 and 0.835, respectively, which are higher than those of SLIC algorithm's 0.743 and 0.749. The VI value of the DPC-IS algorithm under ODS is 1.892. The VI value of the SLIC algorithm is 2.257. The VI value of the PDC algorithm under OIS is 2.074. The VI value of the SLIC algorithm is 2.420. The SC values of DPC-IS and SLIC algorithm under ODS are 0.564 and 0.508, respectively. The SC values under OIS are 0.588 and 0.514. From the table, DPC-IS algorithm has good segmentation performance in image processing and performs well in the field of Visual communication.

TABLE I. PRI, VI AND SC RESULTS OF TWO ALGORITHMS

Evaluating indicator	Optimal threshold	DPC-IS	SLIC
PRI	ODS	0.831	0.743
	OIS	0.835	0.749
VI	ODS	1.892	2.257
	OIS	2.074	2.420
SC	ODS	0.564	0.508
	OIS	0.588	0.514

B. *Performance Analysis of FasterR-CNN Algorithm in Image Detection*

To verify the availability, of FastR-CNN in image detection, FastR-CNN algorithm, R-CNN algorithm, CNN algorithm, and FastR-CNN algorithm were used for comparative experiments. The performance indicators are accuracy, recall, and F-measure values. The experimental platform is Matlab simulation software.

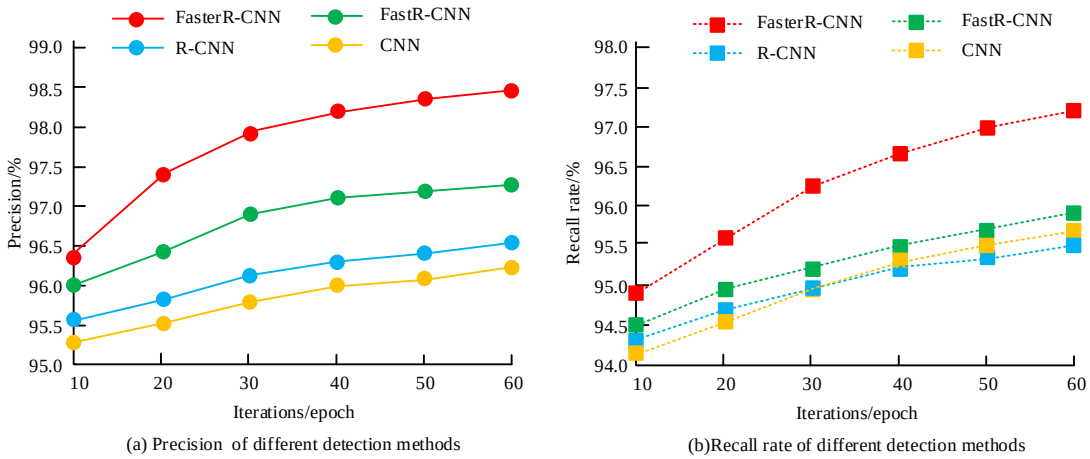

(a) Precision of different detection methods (b)Recall rate of different detection methods

Fig. 9. Precision and recall rate results of four algorithms.

Fig. 9 illustrates the accuracy and recall results of the four algorithms. As the iterations increase, the accuracy and recall of the four algorithms all increase. Fig. 9(a) shows the accuracy variation curves of the four algorithms. When the iteration is 10, the accuracy of the FasterR-CNN is 96.41%. The accuracy rates of FastR-CNN, R-CNN, and CNN algorithms are 96.03%, 95.54%, and 95.32%, respectively. When the iteration is 60,the accuracy of FastR-CNN is 98.49%, which is higher than the 96.87%, 96.35%, and 96.04% of FastR-CNN, R-CNN, and CNN algorithms. Fig. 9(b) shows the recall rate variation curves of the four algorithms. When the number of iterations is 10, the recall rate of FasterR-CNN algorithm is 94.95%. The recall rates of FastR-CNN, R-CNN, and CNN algorithms are 94.48%, 94.31%, and 94.11%, respectively. When the iteration is 60, the recall rate of FastR-CNN algorithm is 97.29%, which is higher than the 95.60%, 95.38%, and 95.24% of FastR-CNN, R-CNN, and CNN algorithms. From the figure, FasterR-CNN has high detection accuracy, which is robust in the field of Visual communication.

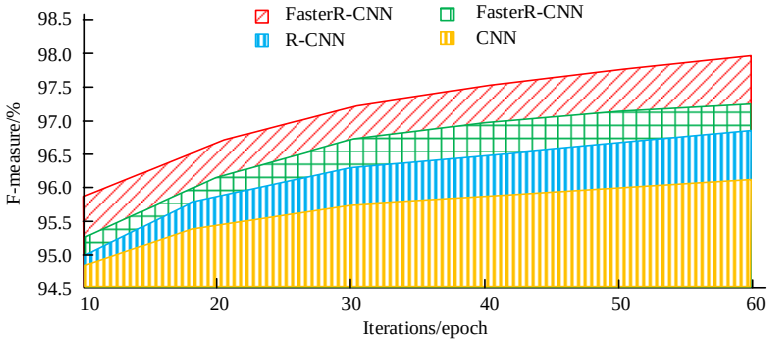

Fig. 10. F-measure results of four algorithms.

The F-measure values of the four algorithms are illustrated in Fig. 10. The F-measure increases with the iteration. When the iteration is 10, the F-measure value of the FasterR-CNN algorithm is 95.90%. The F-measure values of FastR-CNN, R-CNN, and CNN algorithms are 95.26%, 94.99%, and 94.74%, respectively. When the iteration is 60, the F-measure value of the FasterR-CNN algorithm is 97.77%. The F-measure of the FastR-CNN algorithm is 96.87%. The F-measure of the R-CNN algorithm is 96.49%. The F-measure value of the CNN algorithm is 95.51%. From the figure, the FasterR-CNN algorithm has robust performance and good performance.

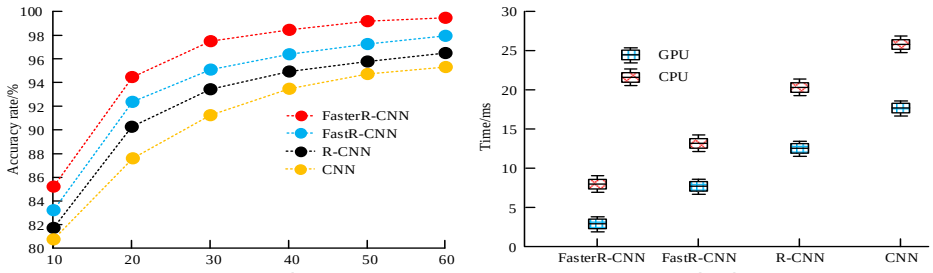

(a) Accuracy results of different algorithms (b) Time consuming of different algorithms in GPU environment and CPU environment.

Fig. 11. Performance results of four algorithms.

Fig. 11 illustrates the experimental results of four algorithms. Fig. 11(a) shows the accuracy results of the four algorithms. As iterations increase, the accuracy of all four algorithms is improving. When the iteration is 60, the accuracy of FastR-CNN is 98.18%, FastR-CNN algorithm is 96.52%, R-CNN algorithm is 95.66%, and CNN algorithm is 93.33%. Fig. 11(b) shows the average time taken by four algorithms to detect a single image in GPU and CPU environments, respectively. The FasterR-CNN algorithm in GPU environment takes 2.94ms. The FastR-CNN algorithm takes 6.28ms. The R-CNN algorithm takes 12.04ms. The CNN algorithm takes 16.21ms. The FasterR-CNN algorithm takes 8.71ms in CPU environment. The FastR-CNN algorithm takes 13.05ms. The R-R-CNN algorithm takes 19.87ms. The R-CNN algorithm takes 25.19ms. The FasterR-CNN algorithm has higher accuracy. The real-time performance is higher than the other three algorithms in both GPU and CPU environments.

V. Conclusion

As a common carrier of Visual communication, image processing with artificial intelligence algorithm has gradually become a development direction. Common image processing technologies include IS technology and image detection technology. Traditional IS technology often only involves the contour information of the image, while ignoring color information, resulting in unclear segmentation levels. Traditional image detection techniques have long computational time consumption, redundant computation, and poor detection efficiency. To address the above issues, the DPC based IS algorithm and FasterR-CNN algorithm are used for image segmentation and detection, respectively. According to the findings, the segmentation accuracy of SLIC is 89.31% and 87.32% respectively in the case of 15% Gaussian noise and 10% Salt-and-pepper noise. The DPC-IS algorithm is 98.13% and 97.89% respectively, significantly higher than SLIC. In the ODS, the PRI and SC values of the PDC algorithm are 0.831 and 0.564, respectively, which are 0.088 and 0.056 higher than the SLIC. The VI value of the PDC is 1.892, which is 0.365 less than the SLIC algorithm. When the iteration is 60, the accuracy, recall, and F-measure values of FastR-CNN algorithm are 98.49%, 97.29%, and 97.77%, respectively, which are 1.62%, 1.69%, and 0.90% higher than FastR-CNN algorithm. In summary, the DPC-IS algorithm and FasterR-CNN algorithm proposed in the study have superior performance, effectively improving segmentation and detection accuracy. However, there are still shortcomings in the research. Firstly, the process of mapping a five dimensional space to a two-dimensional space using maximum mapping may result in data loss, which in turn affects the stability of the algorithm. Secondly, the performance of the proposed method under extreme noise conditions or highly complex image environments still needs further validation. In addition, further efforts are needed to optimize the stability of these algorithms for practical applications. Future research should focus on integrating more complex spatial transformation techniques, such as top-k mapping, to reduce data loss during dimensionality reduction. In addition, exploring the application of these algorithms in dynamic and real-time environments, such as video processing, will provide valuable insights into their scalability. Meanwhile, studying their effectiveness in a wider range of image types, such as medical or satellite images, may also open up new avenues for enhancing visual communication technology.

References

[1] Zomay Z, Keskin B, Ahin C. Grsel letiim Tasarm Blümü rencilerinin Sektrel Logolardaki Renk Tercihleri - Color Preferences of Visual Communication Design Students in Sectoral Logos. OPUS Uluslararası Toplum Araştırmaları Dergisi, 2021, 17(37):4181-4198.

[2] Hidayat I, Ali M Z, Arshad A. Machine Learning-Based Intrusion Detection System: An Experimental Comparison. Journal of Computational and Cognitive Engineering, 2022, 2(2):88-97.

[3] Liu X. Application of cloud-based visual communication design in Internet of Things image. Soft computing: A fusion of foundations, methodologies and applications, 2020, 24(11):8041-8050.

[4] Rai M, Goyal S, Pawar M. An enhanced digital image watermarking technique using DWT-HD-SVD and deep convolutional neural network[J]. International Journal of Critical Computer-Based Systems, 2023, 10(4): 269-286.

[5] Zhang J, Zhou Y, Xia K, Jiang Y, Liu Y. A novel automatic image segmentation method for Chinese literati paintings using multi-view fuzzy clustering technology. Multimedia Systems, 2020, 26(1):37-51.

[6] Amna M, Imen W, Sayadi F E, Atri M. Fast intra-coding unit partition decision in H.266/FVC based on deep learning. Journal of Real-Time Image Processing, 2020, 17(6):1971-1981.

[7] Vani R, Rajan K S. Effective satellite image enhancement based on the discrete wavelet transform. International Journal of Business Information Systems, 2020, 33(4):446-471.

[8] Zhao F, Lu H, Zhao W, Yao L. Image-Scale-Symmetric Cooperative Network for Defocus Blur Detection. IEEE Transactions on Circuits and Systems for Video Technology, 2022, 32(5):2719-2731.

[9] Schonsheck S C, Dong B, Lai R. Parallel transport convolution: Deformable convolutional networks on manifold-structured data[J]. SIAM Journal on Imaging Sciences, 2022, 15(1): 367-386.

[10] Shi Q, Yin S, Wang K, Teng L, Li H. Multichannel convolutional neural network-based fuzzy active contour model for medical image segmentation. Evolving Systems, 2022, 13(4):535-549.

[11] Liu X, Zhang Y, Jing H, Wang L, Zhao S. Ore image segmentation method using U-Net and Res_Unet convolutional networks. RSC Advances, 2020, 10(16):9396-9406.

[12] Ji Y, Jiang X. Active contour model for image segmentation based on salient fitting energy. International Journal of Information and Communication Technology, 2021, 19(2):219-230.

[13] Li Y, Cao G, Wang T, Cui Q, Wang B. A novel local region-based active contour model for image segmentation using Bayes theorem. Information Sciences, 2020, 506:443-456.

[14] Biswas S, Hazra R. Active contours driven by modified LoG energy term and optimised penalty term for image segmentation. IET Image Processing, 2020, 14(13):3232-3242.

[15] Chen J. Automatic Vehicle License Plate Detection using K-Means Clustering Algorithm and CNN. Journal of Electrical Engineering and Automation, 2021, 3(1):15-23.

[16] Vinolin V, Sucharitha M. Taylor-rider-based deep convolutional neural network for image forgery detection in 3D lighting environment. Data technologies and applications, 2022, 56(1):103-131.

[17] Luo J Q, Fang H S, Shao F M, Zhong Y, Hua X. Multi-scale traffic vehicle detection based on faster R–CNN with NAS optimization and feature enrichment. Defence Technology, 2021, 17(4):1542-1554.

[18] Ramaraj P. A Neural Network in Convolution with Constant Error Carousel Based Long Short-Term Memory for Better Face Recognition. Turkish Journal of Computer and Mathematics Education (TURCOMAT), 2021, 12(2):2042-2052.

[19] Joy F, Vijayakumar V. MULTIPLE OBJECT DETECTION IN SURVEILLANCE VIDEO WITH DOMAIN ADAPTIVE INCREMENTAL FAST RCNN ALGORITHM. Indian Journal of Computer Science and Engineering, 2021, 12(4):1018-1026.

[20] Venetis I E, Vasso S, Stathis S, Efstratios G. Multivariable inversion using exhaustive grid search and high-performance GPU processing: a new

perspective. Geophysical Journal International, 2020, 221(2):905-927.

[21] Arieth R M, Anuradha K, Harika B. Congestion Management of CGSTEB Routing protocol Using K-means Algorithm in Wireless Sensor Network. ECS transactions, 2022, 107(1):13147-13154.

[22] Harakannanavar S S, Sameer S R, Kumar V, Behera SK, Amberkar AV, Puranikmath VI. Robust video summarization algorithm using supervised machine learning. Global Transitions Proceedings, 2022, 3(1):131-135.

[23] Shi Y, Shen H. Anomaly Detection for Network Flow Using Immune Network and Density Peak. International Journal of Network Security, 2020, 22(2):337-346.

[24] Chin W L, Zhang Q, Jiang T. Low-complexity neuron for fixed-point artificial neural networks with ReLU activation function in energy-constrained wireless applications. IET communications, 2021, 15(7):917-923.